Journal of Zhejiang University-SCIENCE B (Biomedicine & Biotechnology)
ISSN 1673-1581 (Print); ISSN 1862-1783 (Online)
www.jzus.zju.edu.cn; www.springerlink.com
E-mail: jzus@zju.edu.cn

# Transcriptome sequencing and annotation of the halophytic microalga *Dunaliella salina*[*#]

Ling HONG[†1], Jun-li LIU[1], Samira Z. MIDOUN[1], Philip C. MILLER[†‡2]

([1]*Department of Genetics and Developmental Biology, College of Life Science and Technology, Huazhong University of Science and Technology, Wuhan 430074, China*)

([2]*Systems Biology Research Group, Bioengineering Department, University of California, 9500 Gilman Dr. San Diego, La Jolla, CA 92093, USA*)

[†]E-mail: lhong@mail.hust.edu.cn; pcmiller@eng.ucsd.edu

Received Feb. 21, 2017; Revision accepted Apr. 10, 2017; Crosschecked Sept. 15, 2017

**Abstract:** The unicellular green alga *Dunaliella salina* is well adapted to salt stress and contains compounds (including β-carotene and vitamins) with potential commercial value. A large transcriptome database of *D. salina* during the adjustment, exponential and stationary growth phases was generated using a high throughput sequencing platform. We characterized the metabolic processes in *D. salina* with a focus on valuable metabolites, with the aim of manipulating *D. salina* to achieve greater economic value in large-scale production through a bioengineering strategy. Gene expression profiles under salt stress verified using quantitative polymerase chain reaction (qPCR) implied that salt can regulate the expression of key genes. This study generated a substantial fraction of *D. salina* transcriptional sequences for the entire growth cycle, providing a basis for the discovery of novel genes. This first full-scale transcriptome study of *D. salina* establishes a foundation for further comparative genomic studies.

**Key words:** *Dunaliella salina*; Transcriptome profile; Metabolic processes and adjustment; Regulatory metabolism; Salt stress

http://dx.doi.org/10.1631/jzus.B1700088 **CLC number:** Q36

## 1 Introduction

The unicellular green alga *Dunaliella salina* is well-known for its exceptional capacity to survive in hyper-saline environments due to the rapid accumulation of various osmolytes. As the main producer of natural β-carotene, *D. salina* is widely used for food, nutritional supplements, and cosmetics (Sathasivam *et al.*, 2012). Large amounts of β-carotene are produced by modifying environmental conditions (Mogedas *et al.*, 2009; Tian and Yu, 2009). However, under stress, the cell division of *D. salina* is retarded and cell growth is restricted (Rad *et al.*, 2011), making it difficult to cultivate *D. salina* on a large-scale.

Several thousand expressed sequence tags (ESTs) of *D. salina* generated by traditional sequencing methods have been included in GenBank (National Center for Biotechnology Information (NCBI)) (Alkayala *et al.*, 2010; Zhao *et al.*, 2011). However, the metabolic pathways of prospective commercial compounds in *D. salina* are not well known. Due to the insufficient coverage of less-abundant transcripts (Wang *et al.*, 2010), it is necessary to explore the development and evolution of this organism using genomic, transcriptomic, and proteomic approaches. With a better understanding of the metabolic processes and genetic information of the species, genetic manipulation may potentially enhance the quality and quantity of feedstock. Using a transcriptomic approach,

‡ Corresponding author

* Project supported by the National High-Tech R&D Program (863) of China (No. 2007AA09Z449)

# Electronic supplementary materials: The online version of this article (http://dx.doi.org/10.1631/jzus.B1700088) contains supplementary materials, which are available to authorized users

ORCID: Ling HONG, http://orcid.org/0000-0001-9328-3369

the oleaginous marine alga *D. tertiolecta* was investigated to identify the pathways and genes involved in lipid synthesis, which has potential application in biofuel production (Rismani-Yazdi *et al.*, 2011). The complete organelle (chloroplast and mitochondrial) genomes of *D. salina* were reported recently (Smith *et al.*, 2010). Using complementary DNA (cDNA) microarrays, Kim (2010) investigated the genes (accession number GSE10271) which are important for the growth for *D. salina* under extremely low or high salinities. However, the genome annotation of *D. salina* is far from being completely understood.

For species without a reference genome, mRNA-sequencing technology can detect transcripts corresponding to the existing genomic sequences (Xu *et al.*, 2012) and provide abundant information for a wide range of biological studies (Surget-Groba and Montoya-Burgos, 2010; Liu *et al*., 2015). In this study, we first characterized the transcriptomic database of *D. salina* during the adjustment, exponential and stationary growth phases, and performed transcriptome annotation with a special focus on stress-related compounds. Gene expression under salt stress was verified using relative real-time polymerase chain reaction (PCR).

## 2 Materials and methods

### 2.1 Plant materials and mRNA isolation

*D. salina* strain 435 was obtained from the Freshwater Algae Culture Collection at the Institute of Hydrobiology (FACHB-collection), Chinese Academy of Sciences, Wuhan, China. The cells were cultured in *Dunaliella* medium (DM) in a GXZ-1000A type incubator (Dongnan Instrument Co., Ltd., Ningbo, Zhejiang, China) (Liu *et al.*, 2014).

For mRNA isolation, cells were harvested at different phases of their growth cycle: 30 d (adjustment phase), 80 d (exponential growth phase), and 120 d (stationary phase), using a Legend Micro 17R micro-centrifuge (Thermo Electron, Pittsburgh, PA, USA) at 1500*g* and 4 °C for 5 min. The sediments were lysed using TRIzol reagent (Invitrogen Life Technologies Inc., Carlsbad, CA, USA) to isolate total RNA. Following the instructions of NEBNext Poly(A) mRNA Magnetic Isolation Module Dynabeads® Oligo$(dT)_{25}$ (New England Biolabs, MA, USA), mRNA was isolated and then randomly fragmented by incubation at an elevated temperature (94 °C) in the presence of divalent cations ($Mg^{2+}$).

### 2.2 Construction of a strand-specific cDNA library and transcriptome sequencing

A strand-specific cDNA library was constructed and the paired-end transcriptome was sequenced by the NovoGene Biological Information Technology Co., Ltd. (Beijing, China). All sequencing reads were submitted to the Short Read Archive (SRA) of the NCBI, and can be accessed under accession number SRR1036662.

### 2.3 Raw read analysis and de novo assembly of transcripts

The raw data (raw reads) obtained by sequencing the cDNA library were filtered for reads containing adapters, reads containing poly-N (N ≥10%), and low-quality reads, using Perl scripts (Novogene, Beijing, China). At the same time, the quality 20 (Q20), quality 30 (Q30), GC-content, and duplication sequence level of the clean data were calculated. All the downstream analyses were based on the clean, high-quality data.

The clean reads were first assembled into gene clusters using the Trinity v2012-10-05 program (Grabherr *et al.*, 2011) with the settings: min_kmer_cov set to 2 and all other parameters set to default. Then, all long sequences generated by the Trinity program were assembled into contigs and singletons using CodonCode Aligner 5.0.2 with all parameters set to default.

### 2.4 Functional annotation of unique sequences

For sequence similarity alignment, the *D. salina* unique sequences (uniseqs; contigs and singletons of the CodonCode Aligner results) were annotated using BLAST 2.2.27+ with a cutoff E-value of $\leq 10^{-5}$. The hmmscan of the HMMER 3.0 package was also used to predict the homologous conserved domains by searching the PFAM (protein families) database. Furthermore, uniseqs were functionally assigned into euKaryotic Orthologous Groups (KOGs) (Jensen *et al*., 2008). Using BLAST hit gene identifiers (GIs) and gene accessions, Blast2GO v2.5 software was used to process the BLAST matches and annotate them with gene ontology (GO) terms describing biological processes, molecular functions, and cellular components.

Uniseqs with corresponding enzyme commission (EC) numbers with a cutoff E-value of $\leq 10^{-5}$ were mapped into the Kyoto encyclopedia of genes and genomes (KEGG) database using KEGG Mapper. Then, uniseqs processed by the KEGG automatic annotation server (KAAS) were used to reconstruct the KEGG pathways with KAAS results containing KEGG Orthology (KO) assignments, and the basic rate interface transmission extension (BRITE) hierarchies (Moriya *et al.*, 2007). Hence, uniseqs were categorized according to their role in the KEGG pathways.

### 2.5 Analysis of gene expression level under osmotic stress

To evaluate the effects of osmotic stress on uniseqs, the expression level of a transcript was quantified as reads per kilobase (kb) of the transcript per million mapped reads of the transcriptome (RPKM) (Mortazavi *et al.*, 2008). For each uniseq, the RPKM was calculated based on the formula: RPKM=$a/(b\times c)$, where $a$ represents the number of reads in each de Brujin graph, $b$ represents the number of the total reads (millions), and $c$ represents the uniseq length (kb).

To test the expression levels of key genes involved in the metabolic processes under salt stress, relative quantitative PCR (qPCR) was used to assess the mRNA amount in *D. salina*. We chose algae in the logarithmic phase of growth in DM medium (1.5 mol/L NaCl) as normal cells. The cells were treated by hypo salinity (0.5 mol/L NaCl) and hyper salinity (4.5 mol/L NaCl) for 2 h, and then lysed using TRIzol reagent (Invitrogen Life Technologies Inc., Carlsbad, CA, USA) to isolate total RNA. The co-isolated residual genomic DNA within the total RNA was removed using an RNase-freed DNase 1 enzyme (Promega Co., Madison, WI, USA). The integrity of the total RNA was assessed using formaldehyde agarose gel electrophoresis, and RNA quantity was determined by NanoDrop 2000 spectrophotometer measurements (Thermo Scientific, DE, USA). Relative qPCR was performed with the ABI PRISM® 7900 Real-Time PCR System (Applied Biosystems, CA, USA) using the FastStart Universal SYBR Green Master (ROX; Roche, Basel, Switzerland). The following actin primers were used for endogenous control: 5'-ACCACACCTTCTTCAACGA-3' and 5'-GGATGGCTACATACATGGCA-3' (Chen *et al.*, 2011). Other selected genes involved in the metabolic processes in *D. salina* were analyzed using the primers shown in Table S1. Three experiments were carried out in parallel and the results were calculated based on the mean of the three results.

### 2.6 Statistical analysis

Data are expressed as mean±standard deviation (SD). Statistical analysis of the results was performed using the Student's *t*-test algorithm. $P<0.05$ was set as the level of significant difference.

## 3 Results

### 3.1 Sequencing and de novo assembly of the *D. salina* transcriptome

We constructed a strand-specific cDNA library of pooled RNA of *D. salina* at different growth phases (adjustment phase, logarithmic phase, and stationary phase) to analyze the metabolic processes. The paired-end in-depth sequencing of the cDNA library generated 30445912 (about 5.86 gigabases (Gb)) raw reads with an average length of 200 bp. The statistics of sequencing data quality is presented in Table 1. A total of 29326716 (96.32%) high-quality reads were obtained after filtering the 82128 adapters, removing the 4085 sequences with unknown bases (N >10%) and trimming 1032983 low-quality reads (reads containing more than 50% of bases with a Phred quality score of ≤5).

The high-quality clean reads were assembled de novo into 73443 gene clusters using the Trinity v2012-10-05 program. About 75.4% (55412) of the reads were found to comprise only one sequence

**Table 1 Statistics of sequencing data quality from *D. salina***

| Raw read | Base number (Gb) | Length (bp) | Error (%) | Q20 (%)[1] | Q30 (%)[2] | GC content (%) |
|---|---|---|---|---|---|---|
| 30445912 | 5.86 | 200 | 0.04 | 96.83 | 90.89 | 52.77 |

[1] The error rate of bases with Phred quality score of ≤20 less than 0.01; [2] The error rate of bases with Phred quality score of ≤30 less than 0.001

(Fig. 1a) and the remaining 24.6% (18031) covered 2 to 156 sequences, with 3286 gene clusters having more than five sequences (Fig. 1b). The longest sequence in each de Brujin graph representing the corresponding gene cluster was retrieved and considered as a Trinity unique sequence (Trinity uniseq). Using this criterion, 73443 Trinity uniseqs were generated, with a mean length of 664 bp (ranging from 201 to 15085 bp; Fig. 1c).

The 50406 (68.63%) overlapping sequences of 73443 Trinity uniseqs were further assembled into 16783 contigs using CodonCode Aligner 5.0.2 (CodonCode Co., USA) with parameters set to default.

The coverage depth for contigs (Fig. 1d) ranged from 2 to 29 bp with an average length of 1409 bp (Fig. 1e). The N50 indicates that 50% of the assembled bases were incorporated into contigs longer than 1727 bp (N50=1727 bp). The remaining 23037 Trinity uniseqs could not be assembled into contigs and were defined as singletons, of which 18240 (79.18%) were less than 500 bp. The contigs and singletons represent the transcriptome of *D. salina* with a total of 39820 unique sequences (uniseqs).

### 3.2 Functional annotation of the *D. salina* transcriptome

Based on the similarity of sequence alignment, a total of 12981 (32.57%) uniseqs (9143 contigs and 3838 singletons) had significant BLASTx matches with the non-redundant protein (NR) databases and Swiss-Prot (SP) database. In addition, about 1901 (4.77%) uniseqs had significant BLASTn matches

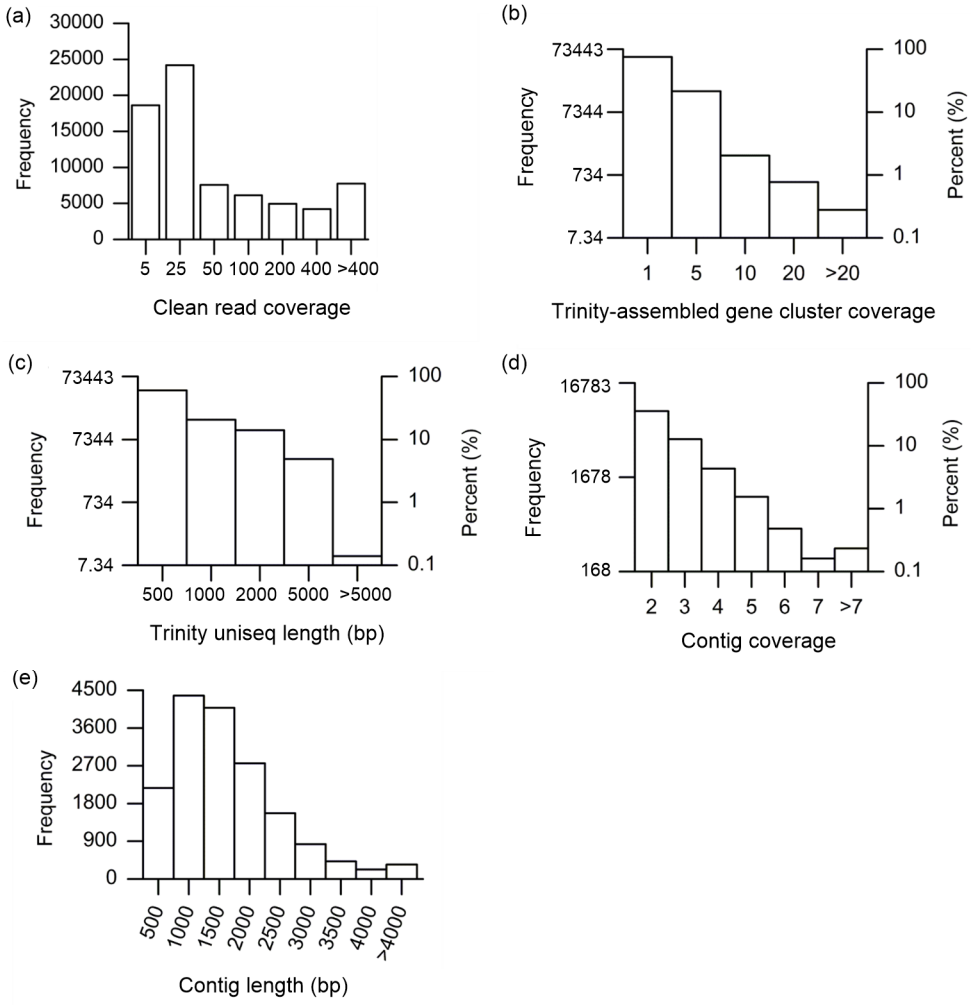


**Fig. 1 Overview of the sequencing and assembly of *D. salina* transcriptome**

(a) Distribution of clean read coverage; (b) Distribution of Trinity-assembled gene cluster coverage; (c) Size distribution of Trinity uniseqs; (d) Distribution of contig coverage; (e) Size distribution of the contig length

with the nucleotide (NT) database (Table S2), of which 1739 uniseqs were found with BLASTx matches. In brief, a total of 13143 (33.01 %) uniseqs (9206 contigs and 3937 singletons) were identified through BLAST matches (Table S2).

According to the species taxonomy, the top hits of the BLAST annotated uniseqs were further clustered into five categories including "Plants", "Animals", "Fungi", "Prokaryotes", and "Viruses" (Fig. 2a). Since there were only five virus species in the "Viruses" category, that category is not shown in Fig. 2a. Most of the 131 plant species had 10599 (80.68%) genes similar to those of *D. salina* (Table S3). Among them, 33.59% species belonged to green algae, predominantly *Volvox carteri* and *Chlamydomonas* (Fig. 2b). In addition, 1326 (10.09%) uniseqs of *D. salina* were shared by 369 prokaryotes, of which 57.32% were shared with *Halomonas*, 894 uniseqs were shared with 264 animal species, and 313 (2.38%) with 138 fungal species.

The uniseqs were further annotated using the hmmscan program to find the conserved domain in the PFAM database. Finally, 18182 uniseqs (45.66%, Table S2) were found, which had 4180 conserved domains. To further evaluate the completeness of the *D. salina* transcriptome, 8908 (22.37%) of the above uniseqs were assigned into 11353 KOG functions with 26 clusters (Fig. S1). A total of 22111 uniseqs (13455 contigs and 8656 singletons) were annotated by the BLAST, PFAM, and KOG databases (Table S2).

Using Blast2GO v2.5 software, a total of 18963 uniseqs (47.62%) were assigned into GO terms describing biological processes (BP), molecular functions (MF), and cellular components (CC) as shown in Fig. S2. Of the GO terms for annotated uniseqs, 5260 uniseqs (3837 contigs and 1423 singletons) were assigned EC numbers (Table S2). Apart from 1872 of the 5260 uniseqs that could not be mapped into any pathway, 6.4% were annotated with biological processes (Fig. S3) using the KEGG mapper (Huson *et al.*, 2011), and were analyzed further for metabolic processes of *D. salina*, with detailed descriptions of the stress-related metabolic compounds (osmolytes and polyamines) and carotenoid metabolic compounds, as described below.

### 3.3 Metabolic processes in *D. salina*

#### 3.3.1 Osmolyte metabolism in *D. salina*

Using the de novo assembly and functional annotation of the *D. salina* transcriptome, we completed the metabolic pathway of glycerol (Fig. 3a). The identified enzymes are shown in Table S4 and the sequences in Data S1. The best hits of their BLAST results are shown in Table S5. An important three-carbon metabolic intermediate for glycerol metabolism is dihydroxyacetone phosphate (DHAP), a product of glycolysis. Nicotinamide adenine dinucleotide ($NAD^+$)-dependent glycerol-3-phosphate dehydrogenase 1 (GPD1) catalyzes glycerol metabolism, which converts DHAP to glycerol-3-phosphate (GLP). Hyperosmotic stress can relieve the inhibition of GPD1 function and activate GPD1 to synthesize GLP (Brewster and Gustin, 2014). GLP is then dephosphorylated by GLP phosphatase 1 (GPPase 1, EC: 3.1.3.21) to form glycerol. Glycerol can also be synthesized by the reduction of dihydroxyacetone (DHA) through catalysis by dihydroxyacetone reductase (DHR, EC: 1.1.1.156). Excess glycerol in

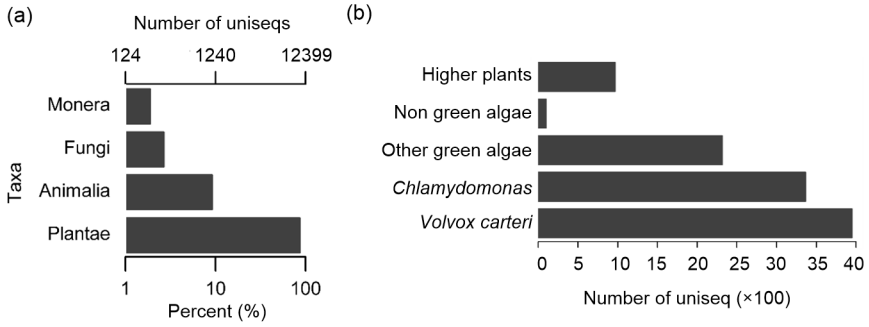


**Fig. 2 Top-hit species distribution of BLAST results of *D. salina* uniseqs**

(a) Number of top-hit species of BLAST results assigned with the "Plant", "Animal", "Fungi", and "Prokaryote" categories. (b) Percent distribution of the top seven green algae (*Volvox carteri*, *Chlamydomona*, *Coccomyxa*, *Chlorella*, *Dunaliella*, *Auxenochlorella*, and *Micromonas*), remaining algae and higher plants in the plant category

cells exposed to hypo-saline stress is degraded to maintain lower osmotic pressure. This reaction is catalyzed by DHR to produce DHA (Chen and Jiang, 2009), followed by phosphorylation with dihydroxyacetone kinase (DAK, EC: 2.7.1.29) to regenerate the three-carbon metabolic intermediate DHAP.

In addition to glycerol, proline (Pro) is another osmolyte accumulated in *D. salina* during the process of adaptation. Pro acts both as a protective agent and a free-radical scavenger in the cytosol (Venekamp, 2006); however, its metabolism has not been analyzed. According to the functional annotation of the *D. salina* transcriptome, the metabolic pathway of Pro was reconstructed (Fig. 3b). The identified enzymes are shown in Table S4, with average transcript levels of 3.29. Their sequences and the best hit of their BLAST results are shown in Data S1 and Table S5. Pro can be synthesized from either glutamine (Glu) or ornithine via the molecule δ-1-pyrroline-5-carboxylate (P5C). Glu is phosphorylated by the enzyme glutamate 5-kinase (proB, EC: 2.7.2.11) to form glutamate-phosphate (GluP) products. Subsequently, it is reduced by glutamate-5-semialdehyde dehydrogenase (GSADH, EC: 1.2.1.41) into glutamate-5-semialdehyde (GSA). These two reactions can also be catalyzed directly by an enzyme, δ-1-pyrroline-5-carboxylate synthetase (P5CS, EC: 2.7.2.1, 1.2.1.41), which is the rate-limiting step for Pro biosynthesis (Deng *et al.*, 2013). This enzyme has both the kinase and γ-glutamyl phosphate reductase domains. One uniseq with two transcripts was identified in the *D. salina* transcriptome. GSA can also be synthesized by transferring the $NH_2$ groups from ornithine to 2-oxo acid. This reaction is catalyzed by ornithine-oxo-acid transaminase (OAT, EC: 2.6.1.13) which was expressed with four transcripts (Table S4). GSA is then spontaneously cyclized to form P5C. Finally, P5C is reduced to Pro by the enzyme pyrroline-5-carboxylate reductase (P5CR, EC: 1.5.1.2), which dehydrogenates $H^+$ from nicotinamide adenine dinucleotide phosphate (NAPDH). In reverse, enzymes related to Pro catabolism were also identified (Table S4), including proline dehydrogenase (PDH, EC: 1.5.99.8) and 1-pyrroline-5-carboxylate dehydrogenase (P5CDH, EC: 1.5.1.12). PDH catalyzes the dehydrogenation of Pro to form P5C, whereas P5CDH converts GSA to Glu.

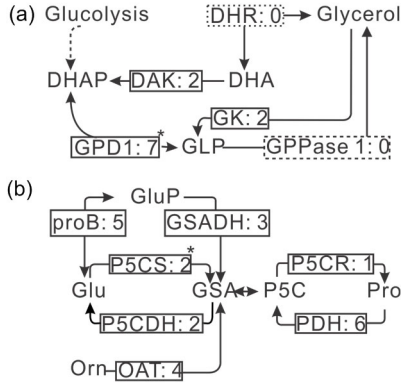


**Fig. 3 Osmolyte metabolic pathways reconstructed based on the de novo assembly and annotation of *D. salina* transcriptome**

(a) Reconstruction of the glycerol metabolic pathway. Enzymes identified and unidentified are shown in the solid and dashed boxes, respectively, and include: DAK (EC: 1.7.1.29), dihydroxyacetone kinase; DHR (EC: 1.1.1.156), dihydroxyacetone reductase; GPD1 (EC: 1.1.1.8), nicotinamide adenine dinucleotide ($NAD^+$)-dependent glycerol-3-phosphate dehydrogenase 1; GK (EC: 2.1.1.30), glycerol kinase; GPPase 1 (EC: 3.1.3.21), glycerol-3-phosphate phosphatase 1. (b) Reconstruction of proline metabolic pathway. Enzymes identified are shown in the solid boxes and include: proB (EC: 2.7.2.11), glutamate 5-kinase; GSADH (EC: 1.2.1.41), glutamate-5-semialdehyde dehydrogenase; P5CS (EC: 2.7.2.1, 1.2.1.41), δ-1-pyrroline-5-carboxylate synthetase; P5CDH (EC: 1.5.1.12), 1-pyrroline-5-carboxylate dehydrogenase; P5CR (EC: 1.5.1.2), pyrroline-5-carboxylate reductase; PDH (EC: 1.5.99.8), proline dehydrogenase; OAT (EC: 2.6.1.13), ornithine-oxo-acid transaminase. The digits behind the colon (:) in each rectangle represent the number of assigned transcripts of enzymes. Key enzymes are shown with a superscript symbol (*) next to the box. DHA, dihydroxyacetone; DHAP, dihydroxyacetone phosphate; GLP, glycerol-3-phosphate; Glu, glutamine; GluP, glutamate-phosphate; Orn, ornithine; GSA, glutamate-5-semialdehyde; P5C, δ-1-pyrroline-5-carboxylate; Pro, proline

### 3.3.2 Polyamine biosynthetic pathway in *D. salina*

Polyamines, including putrescine (Put), spermidine (Spd), and spermine (Spm), are low molecular aliphatic nitrogen compounds found in all living organisms. There are two routes (arginine and ornithine routes) to synthesize putrescine (Put) in *Chlamydomonas reinhardtii*, a relative of *Dunaliella*. These have been investigated intensively and the results show that the ornithine route controls this process with the key enzyme ornithine decarboxylase (ODC, EC: 4.1.1.17) (Voigt *et al.*, 2000). Through the functional annotation of the transcriptome, two uniseqs coding for *N*-carbamoylputrescine amidase (aguB,

EC: 3.5.1.53) and ODC were identified (Table S4). Although arginine decarboxylase (speA, EC: 4.1.1.19) and agmatine deiminase (Adase, EC: 3.5.5.12) were not found in the *D. salina* transcriptome, the identification of aguB implies that *D. salina* might possess these two routes. Using the information from the assembly and annotation of the *D. salina* transcriptome, the polyamine metabolic pathway was reconstructed (Fig. 4). Enzymes involved in the polyamine biosynthetic pathway are shown in Table S4. Their sequences and the best hits of their BLAST results are shown in Data S1 and Table S5 individually. Arginine is decarboxylated by speA to form agmatine (Agm) products. Then, with the catalyzation of the speB enzyme or the aguB and Adase to synthesize Put. Then, Put is successively attached to the aminopropyl groups from the molecule decarboxylated *S*-adenosylmethionine (dcAdoMet) in two-step reactions. They are catalyzed by spermidine synthase (SPDS, EC: 2.5.1.16) and spermine synthase (SPS, EC: 2.5.1.22), with the production of Spd and Spm. Aminopropyl is produced by the enzyme *S*-adenosylmethionine decarboxylase (dsAM, EC: 4.1.1.50) from *S*-adenosyl-L-methionine (AdoMet). Heterologous expression of SPDS from *D. salina*

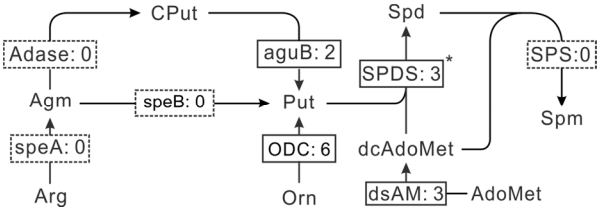


**Fig. 4 Polyamine biosynthetic pathway reconstructed based on the de novo assembly and annotation of *D. salina* transcriptome**

Enzymes identified and unidentified are shown in the solid and dashed boxes, respectively, and include: speA (EC: 4.1.1.19), arginine decarboxylase; Adase (EC: 3.5.3.12), agmatine deiminase; speB (EC: 3.5.3.11), agmatinase; aguB (EC: 3.5.1.53), *N*-carbamoylputrescine amidase; ODC (EC: 4.1.1.17), ornithine decarboxylase; dsAM (EC: 4.1.1.50), *S*-adenosylmethionine decarboxylase; SPDS (EC: 2.5.1.16), spermidine synthase; SPS (EC: 2.5.1.22), spermine synthase. The digits behind the colon (:) in each box represent the number of assigned transcripts of enzymes. Key enzyme is shown with a superscript symbol (*) next to the box. Arg, arginine; Agm, agmatine; CPut, carbamoyl-putrescine; Put, putrescine; AdoMet, *S*-adenosyl-L-methionine; DcAdoMet, *S*-adenosyl-metioninamine; Orn, ornithine; Spd, spermidine; Spm, spermine

may confer tolerance to high salt stress in *Escherichia coli* (Liu *et al.*, 2014).

### 3.3.3 Carotenoid biosynthetic pathway in *D. salina*

Based on the annotation of the *D. salina* transcriptome, carotenogenesis-relevant enzymes were identified (Table S4). Their sequences and the best hits of the BLAST results are shown in Data S1 and Table S5 individually. The carotenogenesis pathway was reconstructed (Fig. 5). Four precursors, geranylgeranyl-phosphates (GGPPs), are condensed to form phytoene, the basic precursor of all carotenoids, and catalyzed by the enzyme phytoene synthase (PSY, EC: 2.5.1.32). Usually, this rate-limiting step is regulated through heterologous overexpression of this gene or environmental modification to enhance carotenoid production (Steinbrenner and Linden, 2001; Couso *et al.*, 2011). Previous studies indicated that this gene is duplicated in the genome sequences in *D. salina* (Tran *et al.*, 2009). Through the de novo assembly of the transcriptome, PSY with three transcripts was identified in *D. salina* with an RPKM of 31.53. Next, phytoene is converted to lycopene with step-wise desaturations by four enzymes: 15-*cis*-phytoene desaturase (PSD, EC: 1.3.5.5), δ-carotene isomerase (ZCI, EC: 5.2.1.12), δ-carotene desaturase (ZDS, EC: 1.3.5.6), and prolycopene isomerase (PLI, EC: 5.2.1.13). Lycopene is then cyclized to carotenes and their derivatives. Three lycopene cyclases were identified, including lycopene β-cyclase (LcyB, EC: 5.5.1.19), lycopene cyclase CruP (CruP), and lycopene ε-cyclase (LcyE, EC: 1.14.13.129). LcyB and CruP catalyze the biosynthesis of α-carotene, β-carotene, and γ-carotene, while LcyE catalyzes the formations of δ-carotene and ε-cyclase. As the main source for natural β-carotene production, *Dunaliella* has been developed to accumulate β-carotene through environmental modification (Mogedas *et al.*, 2009). CruP cannot affect the production of cyclized carotenoids under photo-inhibitory stress and protects against reactive oxygen species (ROS) in oxygenic photosynthetic organisms, providing a unique target to develop algae for food and cosmetics (Bradbury *et al.*, 2012). There were four transcripts coding the CruP enzyme (Table S4).

Carotene derivatives are synthesized by hydroxylation or epoxidation in *D. salina.* There were three hydroxylases identified in the *D. salina* transcriptome,

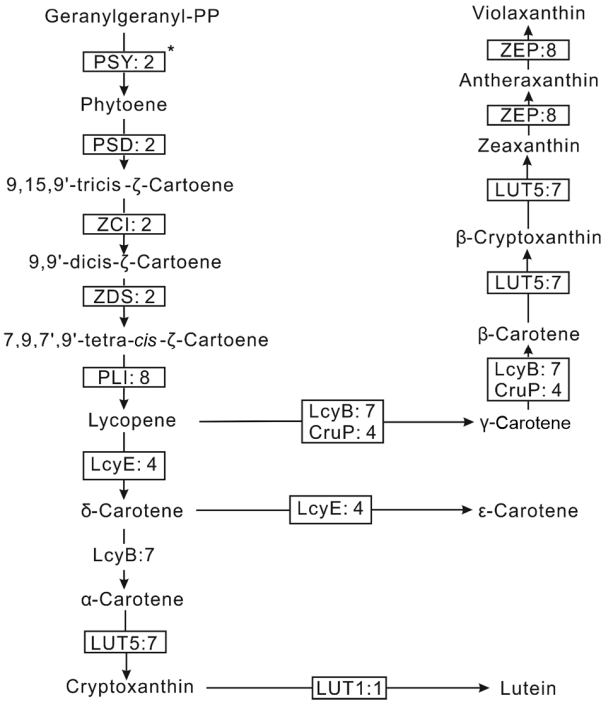


**Fig. 5 Carotenoid biosynthetic pathway reconstructed based on the de novo assembly and the functional annotation of *D. salina* transcriptome**

Enzymes identified are shown in the solid boxes, and include: PSY (EC: 2.5.1.32), phytoene synthase; PSD (EC: 1.3.5.5), 15-*cis*-phytoene desaturase; ZCI (EC: 5.2.1.12), δ-carotene isomerase; ZDS (EC: 1.3.5.6), δ-carotene desaturase; PLI (EC: 5.2.1.13), prolycopene isomerase; LcyB (EC: 5.5.1.19), lycopene β-cyclase; CruP, lycopene cyclase CruP; LUT5 (EC: 1.14.−.−), cytochrome P450, family 97, subfamily A (β-ring hydroxylase); LcyE (EC: 5.5.1.18), lycopene ε-cyclase; ZEP (EC: 1.14.13.90), zeaxanthin epoxidase; LUT1 (EC:1.14.99.45), carotene ε-monooxygenase. The digits behind the colon (:) in each rectangle represent the number of assigned transcripts of enzymes. Key enzyme is shown with a superscript symbol (*) next to the box

including cytochrome P450 enzyme LUT5 (EC: 1.14.−.−), β-carotene hydroxylase (CrtZ, EC: 1.14.13), and carotene ε-monooxygenase (LUT1, EC: 1.14.13.90). They catalyze the formations of zeaxanthin, zeinnxanthin, α-cryptoxanthin, β-cryptoxanthin, and lutein. Finally, the zeaxanthin epoxidase (ZEP, EC: 1.14.13.90) catalyzes antheraxanthin and violaxanthin biosynthesis with the substrate zeaxanthin.

The *D. salina* transcriptome presented here includes all of the enzymes required for carotenoid biosynthesis. The reconstructed pathway is consistent with those proposed for plants (Kim *et al.*, 2009) and algae (Steinbrenner and Linden, 2001; Ramos *et al.*, 2011).

### 3.4 Protective responses of *Dunaliella*: metabolic adjustments

Metabolite adjustment is a protective response of *Dunaliella* under high salinity resulting in a large accumulation of osmolytes and other organic solutes (Mishra *et al.*, 2008). To clarify how it impacts metabolic patterns, relative qPCR was used to assess the mRNA abundance of key genes involved in the metabolic processes of osmolytes (*gpd1*, *p5cs*, and *spds*). In our test, *gpd1* had a relatively high expression under salt stress. Genes (*p5cs* and *spds*) from Pro and polyamine metabolism were found with higher expression under hyper- than under hypo-salinity stress (Fig. 6). Therefore, we conclude that environmental shifts could modify this alga through metabolic adjustments by regulation of the corresponding key genes.

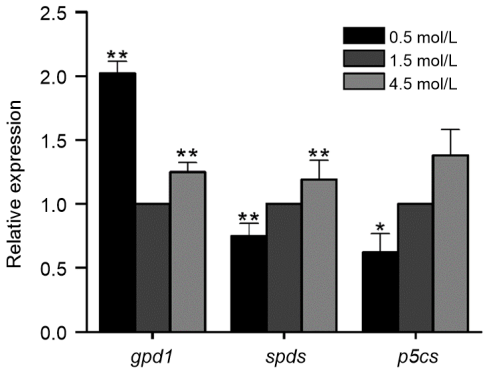


**Fig. 6 Analyses of relative expression levels of key genes in *D. salina* metabolic processes**

Student's *t*-test was used to check the significant differences. * indicates significant difference between salinity stress and control ($P$<0.05). ** indicates extremely significant difference between them ($P$<0.01)

## 4 Discussion

As an osmotic solute, glycerol is an essential molecule to counterbalance environmental osmotic pressure. An increase in salinity promotes intracellular glycerol production within two hours to maintain osmotic homeostasis. Cells recover with osmotic stress-induced gene expression and accumulation of proteins 24 h later (Chen and Jiang, 2009). The carbon for glycerol biosynthesis is obtained mainly from photosynthetic products or the degradation of stored polysaccharides with the latter dominating under

increasing salt stress (Goyal, 2007a; 2007b). The key enzyme, GPD1, has two independent functional domains, glycerol-3-phosphate dehydrogenase (G3PDH) and phosphoserine phosphatase (SerB), which localizes in the chloroplast (Cai *et al.*, 2013) and is highly expressed following hyper- or hypo-salinity stress for two hours, same with other results (Chen *et al.*, 2011). Although the enzymes GPD1, DAK, DHR, and GPPase 1 in the glycerol pathway are regulated by salt stress, GPD1 drives the pathway and controls glycerol synthesis (Chen *et al.*, 2012).

As the most diverse and widespread pigments in the chloroplast, carotenoids, including carotene and lutein, are indispensable in light harvesting and energy transfer during photosynthesis and in the protection of the photosynthetic apparatus against photooxidative damage (Varela *et al.*, 2015). *Dunaliella* have an ability to accumulate carotenoids, especially β-carotene located within the chloroplast, under unfavourable conditions (salinity or nutritional deficiency). The new accumulated β-carotene in the plastids is found within newly formed triacylglycerol droplets. It was reported that the formations of these sequestering structures and β-carotene are interdependent (Rabbani *et al.*, 1998). The biosynthesis of carotenoid and triacylglycerol needs the same precursor acyl-CoA. Two acyl-CoA molecules are condensed to generate mevalonate followed by decarboxylation with mevalonate 5-diphosphate decarboxylase to generate isopentenyl diphosphate (IPP). Farnesyl pyrophosphate synthase catalyzes the head-to-tail condensation reaction of dimethylallyl pyrophosphate with two molecules of IPP to form farnesyl pyrophosphate (FPP), which is the important precursor of all sesquiterpenes (Ferriols *et al.*, 2015) such as carotenoids, ergosterol, and coenzyme Q.

The metabolic process of secondary metabolites is on the dynamic balance and metabolic pathways work under precise control (Wang *et al.*, 2012). There are many ways to increase carotenoid production, e.g. by regulation of expression of the key genes, modification of the growth conditions, or screening for mutants with high carotenoid production. Polyamines are involved in stress signaling through intricate crosstalk with abscisic acid (ABA), $Ca^{2+}$ signaling, and other hormonal pathways in plant defense and development (Marco *et al.*, 2011). With regard to Spd and Spm syntheses, three transcripts coding for SPDS were identified, but none was found for SPS. In *C. reinhardtii* cells and other green algae (*Vovles* and *Chlorella*), no intracellular Spm or only trace amounts were detected (Hamana and Matsuzaki, 1982). Excessive Spm uptake blocks the cell cycle, which can be rescued by subsequent addition of spermidine or putrescine (Theiss *et al.*, 2002). In general, *Dunaleilla* greatly accumulates valuable metabolic products, such as β-carotene, but shows a restricted capacity to grow under stress (high light, high salinity, or chilling) (García *et al.*, 2007), which makes large-scale farming of *Dunaliella* challenging. The excessive Spm accumulated in *Dunaliella* under stress may be one of the causes of growth inhibition. A reduction in the substrates for spermine biosynthesis using inhibitors of *S*-adenosylmethionine decarboxylase (dsAM, EC: 4.1.1.50) and SPDS (Theiss *et al.*, 2002) would allow *Dunaliella* to achieve greater economic value in large-scale production under environmental stress.

Our target was to characterize carotenoid metabolism and identify the corresponding enzymes, not to explore the best way to induce carotenogenesis. Although the pathway in *D. salina* may be the same as in other plants and bacteria, even some algae, this is the first time that a metabolic pathway has been constructed in *D. salina* through transcriptomic analysis.

In conclusion, the characterization of these metabolic pathways and identification of the relevant key enzymes may enable the manipulation of *Dunaliella* to produce these valuable metabolites through bioengineering. Most importantly, the first full-scale transcriptome of *D. salina* at a high resolution lays a foundation for further comparative genomic study.

## Compliance with ethics guidelines

Ling HONG, Jun-li LIU, Samira Z. MIDOUN, and Philip C. MILLER declare that they have no conflict of interest.

This article does not contain any studies with human or animal subjects performed by any of the authors.

## References

Alkayala, F., Albionb, R.L., Tillettb, R.L., *et al.*, 2010. Expressed sequence tag (EST) profiling in hyper saline shocked *Dunaliella salina* reveals high expression of protein synthetic apparatus components. *Plant Sci.*, **179**(5):437-449. http://dx.doi.org/10.1016/j.plantsci.2010.07.001

Bradbury, L.M.T., Shumskaya, M., Tzfadia, O., *et al.*, 2012. Lycopene cyclase paralog CruP protects against reactive oxygen species in oxygenic photosynthetic organisms. *Proc. Natl. Acad. Sci. USA*, **109**:E1888-E1897. http://dx.doi.org/10.1073/pnas.1206002109

Brewster, J.L., Gustin, M.C., 2014. Hog1: 20 years of discovery and impact. *Sci. Signal*, **7**(343):re7. http://dx.doi.org/10.1126/scisignal.2005458

Cai, M., He, L.H., Yu, T.Y., 2013. Molecular clone and expression of a $NAD^+$-dependent glycerol-3-phosphate dehydrogenase isozyme gene from the halotolerant alga *Dunaliella salina*. *PLoS ONE*, **8**(4):e62287. http://dx.doi.org/10.1371/journal.pone.0062287

Chen, H., Jiang, J., 2009. Osmotic responses of *Dunaliella* to the changes of salinity. *J. Cell Physiol.*, **219**(2):251-258. http://dx.doi.org/10.1002/jcp.21715

Chen, H., Lao, Y.M., Jiang, J.G., 2011. Effects of salinities on the gene expression of a ($NAD^+$)-dependent glycerol-3-phosphate dehydrogenase in *Dunaliella salina*. *Sci. Total Environ.*, **409**(7):1291-1297. http://dx.doi.org/10.1016/j.scitotenv.2010.12.038

Chen, H., Lu, Y., Jiang, J.G., 2012. Comparative analysis on the key enzymes of the glycerol cycle metabolic pathway in *Dunaliella salina* under osmotic stresses. *PLoS ONE*, **7**(6):e37578. http://dx.doi.org/10.1371/journal.pone.0037578

Conesa, A., Götz, S., García-Gomez, J.M., *et al.*, 2005. Blast2GO: a universal tool for annotation, visualization and analysis in functional genomics research. *Bioinformatics*, **21**(18):3674-3676. http://dx.doi.org/10.1093/bioinformatics/bti610

Couso, I., Vila, M., Rodriguez, H., *et al*., 2011. Overexpression of an exogenous phytoene synthase gene in the unicellular alga *Chlamydomonas reinhardtii* leads to an increase in the content of carotenoids. *Biotechnol. Prog.*, **27**(1):54-60. http://dx.doi.org/10.1002/btpr.527

Deng, G., Liang, J., Xu, D., *et al.*, 2013. The relationship between proline content, the expression level of P5CS ($\Delta^1$-pyrroline-5-carboxylate synthetase), and drought tolerance in tibetan hulless barley (*Hordeum vulgare* var. *nudum*). *Russ. J. Plant Physiol.*, **60**(5):693-700. http://dx.doi.org/10.1134/S1021443713050038

Ferriols, V.M.E.N., Yaginuma, R., Adachi, M., *et al.*, 2015. Cloning and characterization of farnesyl pyrophosphate synthase from the highly branched isoprenoid producing diatom *Rhizosolenia setigera*. *Sci. Rep.*, **5**:10246.

García, F., Freile-Pelegrin, Y., Robledo, D., 2007. Physiological characterization of *Dunaliella* sp. (Chlorophyta, Volvocales) from Yucatan, Mexico. *Bioresour. Technol*., **98**(7):1359-1365. http://dx.doi.org/10.1016/j.biortech.2006.05.051

Goyal, A., 2007a. Osmoregulation in *Dunaliella*, part I: effects of osmotic stress on photosynthesis, dark respiration and glycerol metabolism in *Dunaliella tertiolecta* and its salt-sensitive mutant (HL 25/8). *Plant Physiol. Biochem.*, **45**(9):696-704. http://dx.doi.org/10.1016/j.plaphy.2007.05.008

Goyal, A., 2007b. Osmoregulation in *Dunaliella*, Part II: photosynthesis and starch contribute carbon for glycerol synthesis during a salt stress in *Dunaliella tertiolecta*. *Plant Physiol. Biochem.*, **45**(9):705-710. http://dx.doi.org/10.1016/j.plaphy.2007.05.009

Grabherr, M.G., Haas, B.J., Yassour, M., *et al.*, 2011. Full-length transcriptome assembly from RNA-Seq data without a reference genome. *Nat. Biotechnol.*, **29**(7): 644-654. http://dx.doi.org/10.1038/nbt.1883

Hamana, K., Matsuzaki, S., 1982. Widespread occurrence of norspermidine and norspermine in eukaryotic algae. *J. Biochem.*, **91**(4):1321-1328. http://dx.doi.org/10.1093/oxfordjournals.jbchem.a133818

Huson, D.H., Mitra, S., Ruscheweyh, H.J., *et al.*, 2011. Integrative analysis of environmental sequences using MEGAN4. *Genome Res.*, **21**(9):1552-1560. http://dx.doi.org/10.1101/gr.120618.111

Jensen, L.J., Julien, P., Kuhn, M., *et al*., 2008. eggNOG: automated construction and annotation of orthologous groups of genes. *Nucleic Acids Res*., **36**(Databse issue): D250-D254. http://dx.doi.org/10.1093/nar/gkm796

Kim, J., Smith, J.J., Tian, L., *et al.*, 2009. The evolution and function of carotenoid hydroxylases in *Arabidopsis*. *Plant Cell Physiol.*, **50**(3):463-479. http://dx.doi.org/10.1093/pcp/pcp005

Liu, H., Wu, W., Hou, K., *et al*., 2015. Transcriptome changes in *Polygonum multiflorum* Thunb. roots induced by methyl jasmonate. *J. Zhejiang Univ.-Sci. B (Biomed. & Biotechnol.)*, **16**(12):1027-1041. http://dx.doi.org/10.1631/jzus.B1500150

Liu, J., Zhang, D., Hong, L., 2014. Isolation, characterization and functional annotation of the salt tolerance genes through screening the high-quality cDNA library of the halophytic green alga *Dunaliella salina* (Chlorophyta). *Ann. Microbiol.*, **24**(3):1293-1302. http://dx.doi.org/10.1007/s13213-014-0967-z

Marco, F., Alcázar, R.N., Tiburcio, A.F., *et al.*, 2011. Interactions between polyamines and abiotic stress pathway responses unraveled by transcriptome analysis of polyamine overproducers. *OMICS*, **15**(11):775-782. http://dx.doi.org/10.1089/omi.2011.0084

Mishra, A., Mandoli, A., Jha, B., 2008. Physiological characterization and stress-induced metabolic responses of *Dunaliella salina* isolated from salt pan. *J. Ind. Microbiol. Biot.*, **35**(10):1093-1101. http://dx.doi.org/10.1007/s10295-008-0387-9

Mogedas, B., Casal, C., Forján, E., *et al.*, 2009. β-Carotene production enhancement by UV-A radiation in *Dunaliella bardawil* cultivated in laboratory reactors. *J. Biosci. Bioeng.*, **108**(1):47-51. http://dx.doi.org/10.1016/j.jbiosc.2009.02.022

Moriya, Y., Itoh, M., Okuda, S., *et al.*, 2007. KAAS: an automatic genome annotation and pathway reconstruction

server. *Nucleic Acids Res.*, **35**(Suppl. 2):W182-W185. http://dx.doi.org/10.1093/nar/gkm321

Mortazavi, A., Williams, B.A., McCue, K., *et al.*, 2008. Mapping and quantifying mammalian transcriptomes by RNA-Seq. *Nat. Methods*, **5**(7):621-628. http://dx.doi.org/10.1038/nmeth.1226

Rabbani, S., Beyer, P., Lintig, J.V., *et al.*, 1998. Induced β-carotene synthesis driven by triacylglycerol deposition in the unicellular alga *Dunaliella bardawil*. *Plant Physiol.*, **116**:1239-1248. http://dx.doi.org/10.1104/pp.116.4.1239

Rad, F.A., Aksoz, N., Hejazi, M.A., 2011. Effect of salinity on cell growth and β-carotene production in *Dunaliella* sp. isolates from Urmia Lake in northwest of Ira. *Afr. J. Biotechnol*., **10**(12):2282-2289.

Ramos, A.A., Polle, J., Tran, D., *et al.*, 2011. The unicellular green alga *Dunaliella salina* Teod. as a model for abiotic stress tolerance: genetic advances and future perspectives. *Harmful Algae*, **26**(1):3-20. http://dx.doi.org/10.4490/algae.2011.26.1.003

Rismani-Yazdi, H., Haznedaroglu, B.Z., Bibby, K., *et al.*, 2011. Transcriptome sequencing and annotation of the microalgae *Dunaliella tertiolecta*: pathway description and gene discovery for production of next-generation biofuels. *BMC Genomics*, **12**:148. http://dx.doi.org/10.1186/1471-2164-12-148

Sathasivam, R., Kermanee, P., Roytrakul, S., *et al.*, 2012. Isolation and molecular identification of β-carotene producing strains of *Dunaliella salina* and *Dunaliella bardawil* from salt soil samples by using species-specific primers and internal transcribed spacer (ITS) primers. *Afr. J. Biotechnol.*, **11**(102):16677-16687.

Smith, D.R., Lee, R.W., Cushman, J.C., *et al.*, 2010. The *Dunaliella salina* organelle genomes: large sequences, inflated with intronic and intergenic DNA. *BMC Plant Biol.*, **10**:14. http://dx.doi.org/10.1186/1471-2229-10-14

Steinbrenner, J., Linden, H., 2001. Regulation of two carotenoid biosynthesis genes coding for phytoene synthase and carotenoid hydroxylase during stress-induced astaxanthin formation in the green alga *Haematococcus pluvialis*. *Plant Physiol.*, **125**(2):810-817. http://dx.doi.org/10.1104/pp.125.2.810

Surget-Groba, Y., Montoya-Burgos, J.I., 2010. Optimization of de novo transcriptome assembly from next-generation sequencing data. *Genome Res*., **20**:1432-1440.

Theiss, C., Bohley, P., Voigt, J., 2002. Regulation by polyamines of ornithine decarboxylase activity and cell division in the unicellular green alga *Chlamydomonas reinhardtii*. *Plant Physiol.*, **128**(4):1470-1479. http://dx.doi.org/10.1104/pp.010896

Tian, J., Yu, J., 2009. Changes in ultrastructure and responses of antioxidant systems of algae (*Dunaliella salina*) during acclimation to enhanced ultraviolet-B radiation. *J. Photochem. Photobiol. B*, **97**(3):152-160. http://dx.doi.org/10.1016/j.jphotobiol.2009.09.003

Tran, D., Haven, J., Qiu, W.G., *et al.*, 2009. An update on carotenoid biosynthesis in algae: phylogenetic evidence for the existence of two classes of phytoene synthase. *Planta*, **229**(3):723-729. http://dx.doi.org/10.1007/s00425-008-0866-2

Varela, J.C., Pereira, H., Vila, M., *et al.*, 2015. Production of carotenoids by microalgae: achievements and challenges. *Photosynth. Res.*, **125**:423-436. http://dx.doi.org/10.1007/s11120-015-0149-2

Venekamp, J.H., 2006. Regulation of cytosol acidity in plants under conditions of drought. *Physiol. Plantarum*, **76**(1): 112-117. http://dx.doi.org/10.1111/j.1399-3054.1989.tb05461.x

Voigt, J., Deinert, B., Bohley, P., 2000. Subcellular localization and light-dark control of ornithine decarboxylase in the unicellular green alga *Chlamydomonas reinhardtii*. *Physiol. Plant*, **108**(2000):353-360. http://dx.doi.org/10.1034/j.1399-3054.2000.108004353.x

Wang, X., Xia, X., Huang, F., *et al*., 2012. Genetic modification of secondary metabolite biosynthesis in higher plants: a review. *J. Biotechnol.*, **28**(10):1151-1163 (in Chinese).

Wang, Z., Fang, B., Chen, J., *et al.*, 2010. *De novo* assembly and characterization of root transcriptome using Illumina paired-end sequencing and development of cSSR markers in sweetpotato (*Ipomoea batatas*). *BMC Genomics*, **11**: 726-739. http://dx.doi.org/10.1186/1471-2164-11-726

Xu, D.L., Long, H., Liang, J.J., *et al.*, 2012. De novo assembly and characterization of the root transcriptome of *Aegilops variabilis* during an interaction with the cereal cyst nematode. *BMC Genomics*, **13**:133-141.

Zhao, R., Cao, Y., Xu, H., *et al.*, 2011. Analysis of espressed sequence tags from the green alga *Dunaliella salina* (Chalrophyta). *J. Phycol.*, **47**(6):1454-1460. http://dx.doi.org/10.1111/j.1529-8817.2011.01071.x

## List of electronic supplementary materials

Data S1 Sequences of the genes identified in *D. salina* transcriptome

Table S1 Primers of those selective genes involved in the metabolic processes in *D. salina*

Table S2 Summary of annotation of *D. salina* transcriptome

Table S3 Top-hit species (viridiplantae) list of *D. salina* BLAST-annotated uniseqs

Table S4 Enzymes identified in metabolism of osmolytes (glycerol and proline), polyamines, and carotenoid through annotation of *D. salina* transcriptome

Table S5 The best hit of the highlighted enzymes in the metabolic processes of *D. salina*

Fig. S1 KOG (euKaryotic Ortholog Groups) functional classification of *D. salina* uniseqs

Fig. S2 Gene ontology (GO) annotation of *D. salina* transcriptome

Fig. S3 KEGG functional analyses of *D. salina* uniseqs

## 中文概要

**题　目：盐生海藻杜氏盐藻的转录组测序以及注释**

**目　的：**解析杜氏盐藻代谢过程，主要关注盐胁迫下累积的代谢物（渗透平衡产物、多胺和类胡萝卜素）的代谢。

**创新点：**本研究通过高通量测序产生了大量来自杜氏盐藻整个生长周期的转录组数据，描述了杜氏盐藻在盐胁迫下累积的渗透平衡产物、多胺和类胡萝卜素的代谢过程。另外通过该手段也进一步分析了盐胁迫处理下，抑制精胺合成底物的供应可能会缓解盐藻增殖对胡萝卜素含量的影响。

**方　法：**以来自 3 个不同生长时期的杜氏盐藻为材料，进行大规模转录组测序。在转录组功能注释的基础上，预测了杜氏盐藻盐胁迫下累积的渗透平衡产物（图 3）、多胺（图 4）和类胡萝卜素（图 5）的代谢路径。利用相对定量聚合酶链反应（qPCR）技术构建了相关代谢路径中关键基因的表达谱（图 6）。

**结　论：**通过杜氏盐藻转录组测序共获取了 39820 条单一序列。在功能注释和聚类分析的基础上预测了杜氏盐藻盐胁迫下累积的渗透平衡产物（甘油和脯氨酸）、多胺以及类胡萝卜素的代谢路径。相关代谢途径的关键酶的表达谱分析，说明盐能够调节甘油、脯氨酸以及多胺的代谢过程。抑制精胺合成底物的供应可能会缓解盐藻增殖对胡萝卜素含量的影响。

**关键词：**杜氏盐藻；转录谱；代谢过程与调控；调节机制；盐胁迫